Nuclear Science and Techniques (2024) 35:120
https://doi.org/10.1007/s41365-024-01464-8

Study of baryon number transport dynamics and strangeness conservation effects using Ω-hadron correlations

Wei-Jie Dong[1] · Xiao-Zhou Yu[1] · Si-Yuan Ping[1] · Xia-Tong Wu[2] · Gang Wang[2] · Huan-Zhong Huang[1,2] · Zi-Wei Lin[3]

Received: 8 December 2023 / Revised: 8 March 2024 / Accepted: 8 April 2024 / Published online: 11 July 2024

Abstract
In nuclear collisions at RHIC energies, an excess of Ω hyperons over $\bar{\Omega}$ is observed, indicating that Ω has a net baryon number despite s and $\bar{s}$ quarks being produced in pairs. The baryon number in Ω may have been transported from the incident nuclei and/or produced in the baryon-pair production of Ω with other types of anti-hyperons such as $\bar{\Xi}$. To investigate these two scenarios, we propose to measure the correlations between Ω and K and between Ω and anti-hyperons. We use two versions, the default and string-melting, of a multiphase transport (AMPT) model to illustrate the method for measuring the correlation and to demonstrate the general shape of the correlation. We present the Ω-hadron correlations from simulated Au+Au collisions at $\sqrt{s_{\rm NN}} = 7.7$ and 14.6 GeV and discuss the dependence on the collision energy and on the hadronization scheme in these two AMPT versions. These correlations can be used to explore the mechanism of baryon number transport and the effects of baryon number and strangeness conservation on nuclear collisions.

Keywords Baryon number transport · Strangeness conversation · Correlation · Gluon junction

1 Introduction

Strangeness enhancement was originally proposed as a signature of the quark-gluon plasma (QGP) created in relativistic heavy-ion collisions [1] and has been the subject of intense theoretical and experimental investigations [2–6]. Because the incident protons and neutrons are composed of u and d quarks, the strange quarks observed in the aftermath of a collision can only originate from a pair of $s\bar{s}$ productions. Lattice quantum chromodynamics (QCD) has predicted that the temperature at which the quark-hadron phase transition occurs is approximately 150 MeV. Thus, in the QGP phase, where the temperature is comparable to the s-quark mass, strangeness may be abundantly produced via flavor creation ($qq \to s\bar{s}$, $gg \to s\bar{s}$) and gluon splitting ($g \to s\bar{s}$), leading to an enhanced production of strangeness in the final state [1, 7]. The investigation of multi-strange hyperon production is particularly valuable for studying the equilibration of strangeness in the QGP. For example, the yields of Ω hyperons in heavy-ion collisions have been measured to be significantly higher than those in p+p collisions scaled by the number of participants at the CERN Super Proton Synchrotron (SPS) [8], relativistic heavy ion collider (RHIC) [2, 9], and Large Hadron Collider (LHC) [10, 11]. In addition, many strange hadrons are believed to have small hadronic rescattering cross sections and little contribution from resonance decay [12, 13]. Accordingly, they retain information from the hadronization stage and can be used to probe the phase boundary of the quark-hadron transition [14–22] (Fig. 1).

The RHIC beam energy scan (BES) program searches for a possible critical point in the QCD phase diagram [23], where strangeness production plays a major role [24]. At low BES energies, the measured ratios of anti-baryons to baryons are significantly lower than unity at midrapidities for three hyperons (Λ, Ξ, and Ω). Therefore, these hyperons

✉ Gang Wang
gwang@physics.ucla.edu

✉ Huan-Zhong Huang
huang@physics.ucla.edu

[1] Key Laboratory of Nuclear Physics and Ion-beam Application (MOE), Fudan University, Shanghai 200433, China

[2] Department of Physics and Astronomy, University of California, Los Angeles, CA 90095, USA

[3] Department of Physics, East Carolina University, Greenville, NC 27858, USA

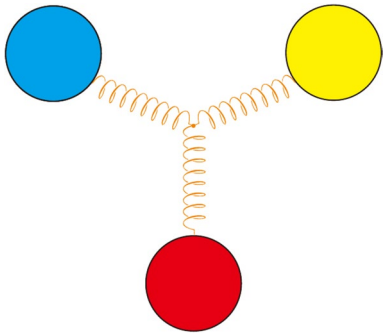

Fig. 1 (Color online) Gluon junction configuration is the Y-shaped gluon field (orange curve) in the structure of the baryon, which is speculated to be the baryon number carrier. The three circles represent valance quarks in a baryon

must have net baryon numbers. Baryon number transport dynamics has been a subject of interest in heavy-ion collision physics since its inception [25–27]. The baryon number in a proton or neutron can be attributed to the valence u and d quarks, each carrying 1/3 of the baryon number. However, in high-energy collisions, valence quarks tend to inherit a significant fraction of the incident nucleon momentum, thus rendering them ineffective in transporting the baryon number from beam rapidities to midrapidities [28, 29]. Previous theoretical calculations have proposed the interactions of topological objects known as gluon junctions, as shown in Fig. 2, which can effectively convey the baryon number over large rapidity gaps in nuclear collisions [30]. Once a gluon junction reaches midrapidities during a nuclear collision, it must emerge as a baryon in the final state, where its flavor is determined by the quark flavors present in the surrounding QGP medium. These exotic dynamics have a particularly discernible effect on the net Ω hyperons, as Ω hyperons consist of three s quarks that must be pair-produced.

The quantum numbers of strangeness and the baryon number are strictly conserved in nuclear collisions, leading to correlations among the particles in the final state. To gain insight into the production dynamics of Ω hyperons, we propose to measure the correlations between Ω and other particles, namely, K^+, $\bar{\Lambda}$, and $\bar{\Xi}^+$, along with their respective anti-particle pairs. By examining the shape and strength of these correlation functions, we illustrate the extent to which we can quantitatively characterize the role of conservation laws in the Ω production dynamics in nuclear collisions. These correlations also provide a means to search for possible exotic dynamics, such as gluon junction interactions, for baryon number transport.

In this study, we use a multiphase transport (AMPT) model [31, 32] to simulate Au+Au collisions at $\sqrt{s_{\rm NN}} = 7.7$ and 14.6 GeV and present the Ω-hadron correlations from these simulations. In Sect. 2, we briefly describe AMPT simulations and analytical methods. The correlation results and discussion are presented in Sect. 3, followed by a summary in Sect. 4.

2 AMPT simulations and analytical methods

2.1 AMPT simulations

To investigate the effects of different hadronization schemes on baryon number transport dynamics, we used both the default and string melting (SM) versions of the AMPT model to simulate Au+Au collisions. The initial phase space is provided by the HIJING model [33–36], which is a Monte Carlo event generator for parton and particle production in high-energy hadronic and nuclear collisions. In the default version of AMPT, minijets and their parent nucleons form excited strings after partonic interactions with minijets, and these strings fragment into hadrons through Lund string fragmentation [37]. In the SM version, strings are converted through the "string melting" mechanism into partons, which subsequently interact during evolution, and the coalescence mechanism is used to combine partons into hadrons. The parton interactions are described by the Boltzmann equation and solved using the ZPC model [38], which includes only two-body elastic scatterings. In the quark coalescence process, the two or three nearest partons (quarks

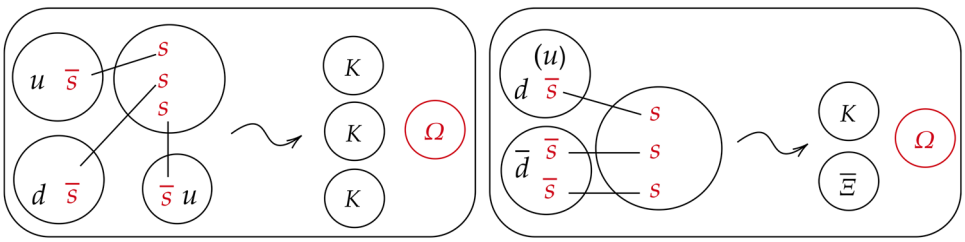

Fig. 2 Schematics of two possible scenarios for Ω^- production based on the quark coalescence picture with strangeness and baryon number conservation. In Scenario 1 (left, general associate production), Ω^- carries the baryon number that initially resides in the u and d quarks from colliding nuclei. In Scenario 2 (right, general pair production), Ω^- does not carry a net baryon number in the production mechanism. Associated production of Ω and kaon in the AMPT default version could have similar qualitative features as those of Scenario 1 in the coalescence picture. The $\bar{\Xi}$ hyperon in the figure is an example of pair production of Ω and $\bar{\Xi}$

and anti-quarks) in phase space recombine to form a meson or baryon. This study uses the AMPT version that strictly conserves the net electric charge, strangeness, and baryon number. We generated more than 50 million minimum bias events of Au+Au collisions at both 7.7 and 14.6 GeV.

2.2 Ω production and conservation of strangeness and baryon number

Ω^- production is governed by both strangeness conservation (SC) and baryon number conservation. In addition, the presence of net Ω hyperons at midrapidities indicates the involvement of baryon number transport (BNT) dynamics. Figure 2 illustrates the two basic scenarios based on the quark coalescence picture for the Ω^- production. In Scenario 1, or the *general associate production* (left side of Fig. 2), three $\bar{s}$ quarks are pair-produced with the three s quarks in Ω^- and may combine with u or d quarks from the incident nuclei to form three kaons. In this case, the Ω^- hyperon does not have an accompanying anti-baryon and carries a fraction of the total net baryon number transported from the colliding nuclei. In exotic dynamics involving gluon junction interactions, the production of three s-$\bar{s}$ pairs may be combined with a gluon junction to yield Ω^-. Consequently, general associate production is inclusive of a possible exotic BNT via gluon junction to the Ω hyperon, whereas valence u/d quarks form the kaons [27]. In the default version, the associated production of Ω and kaons can yield features that are qualitatively similar to the coalescence picture. Therefore, general associate production encompasses contributions from both ordinary physical processes and gluon junction dynamics. The AMPT model in our simulation does not explicitly include gluon junction dynamics. We use Scenario 1, or general associate production, to denote a general process in which a net baryon number is transported to the Ω hyperon regardless of the underlying dynamics. In Scenario 2, or *general pair production* (right side of Fig. 2), the three pair-produced $\bar{s}$ quarks combine with $u(\bar{u})$ or $d(\bar{d})$ quarks to form an anti-hyperon and kaon. For example, $\bar{\Xi}^+(\bar{\Xi}^0)$ and $K^0(K^+)$ can emerge alongside the Ω^- hyperon. In this scenario, the baryon number in Ω^- is balanced by other types of anti-hyperon, and no net baryon number from the incident nuclei is present.

To characterize the numbers of kaons and anti-baryons associated with Ω production, we introduce

$$\Delta N_{\mathrm{A}} \equiv \langle A \rangle_{\mathrm{w.}\Omega^-} - \langle A \rangle_{\mathrm{w.o.}\Omega^-}, \tag{1}$$

where $\langle A \rangle_{\mathrm{w.}\Omega^-}$ and $\langle A \rangle_{\mathrm{w.o.}\Omega^-}$ denote the average numbers of particles A in events with one Ω^- and without any Ω^-, respectively. Here, we assume that all other aspects of the two event classes are the same. Table 1 lists the ΔN_K and $\Delta N_{\bar{B}}$ values expected by the two scenarios, where K represents both K^+ and K^0, and $\bar{B}$ refers to anti-baryons ($\bar{\Lambda}$, $\bar{\Sigma}$, $\bar{\Xi}$, and so on) associated with the Ω^- production. In our study, we chose the beam energies of 7.7 and 14.6 GeV to limit the fraction of Au+Au events that produce multiple Ω ($\bar{\Omega}$) hyperons. Compared with general pair production, general associate production exhibits a stronger Ω^--K correlation and a weaker Ω^--$\bar{B}$ correlation.

2.3 Correlation using the event mixing technique

To divide the combinatorial background, we first analyze the correlations between Ω^- and strange hadrons with traditional normalization using mixed events, which is similar to the scheme used in other analyses (e.g., [39]). The correlation function is expressed as

$$C(k^*) = \mathcal{N} \frac{A(k^*)}{B(k^*)}, \tag{2}$$

where $A(k^*)$ is the same-event distribution, $B(k^*)$ is the mixed-event distribution, and $k^* \equiv \frac{1}{2}|k_1 - k_2|$ is the reduced momentum in the pair rest frame. In addition, $\mathcal{N}$ is the normalization factor determined by matching the same- and mixed-event correlations in the uncorrelated phase space, for example, by requiring $C(k^* > 1\,\mathrm{GeV}/c) = 1$.

The event mixing normalization technique enables the correlation length between two types of particles in momentum space to be investigated by analyzing their distributions. The underlying assumption is that the distribution of mixed events should be equivalent to that of the same events in the absence of any correlation. By dividing this mixed-event background, we can obtain the correlation between the two particles of interest. To achieve meaningful results, selecting an appropriate k^* range for normalization is crucial. Typically, the k^* range with a high counting density is selected for normalization because it provides a reliable background estimate. This method has also been applied to examine the correlation function for Ω^--K^+, Ω^--$\bar{\Lambda}^0$, and Ω^--$\bar{\Xi}^+$ in terms of the relative rapidity and relative transverse momentum. However, with the normalization procedure, this correlation function cannot fully capture the magnitude of multiple kaons correlated with Ω production, nor can it adequately represent the sensitivity of the correlation to the production dynamics.

2.4 Correlations using combinatorial background subtraction

To make the correlation measurement sensitive to the number of associated hadrons, we introduce combinatorial background subtracted (CBS) correlations by taking the difference between the Ω- and $\bar{\Omega}$-hadron correlations, each normalized by the corresponding number of Ω or $\bar{\Omega}$ hyperons. For example, the Ω^--K^+ correlation is defined as

$$C^{\mathrm{CBS}}_{\Omega^-K^+}(k^*) = \frac{\mathrm{d}N_{\Omega^-K^+}/\mathrm{d}k^*}{N_{\Omega^-}} - \frac{\mathrm{d}N_{\bar{\Omega}^+K^+}/\mathrm{d}k^*}{N_{\bar{\Omega}^+}}. \quad (3)$$

Due to the SC in the Ω^--K^+ pairs, this background subtraction approach is intended to extract the main component of the correlation. The opposite-sign pair (Ω^--K^+ or $\bar{\Omega}^+$-K^-) distribution in the first term contains the signal, whereas the same-sign pair distribution in the second term ($\bar{\Omega}^+$-K^+ or Ω^--K^-) models the uncorrelated background. This subtraction scheme is sensitive to the difference in the number of kaons between events with Ω^- and those with $\bar{\Omega}^+$ as well as to the phase-space distribution of the extra kaons. There may be variations in the kinematic phase spaces of these pairs in nuclear collisions, and these effects can be mitigated using this normalization scheme and fine collision centrality bins. Similar approaches have been applied to study the correlations between Ω and other hadrons.

3 Correlation results and discussion

3.1 Strangeness conservation and strange hadron yields

Table 2 lists the AMPT simulations for determining the differences in the numbers of $s\bar{s}$ pairs between events with one Ω^- and those without any Ω^- or $\bar{\Omega}^+$ in the Au+Au collisions at $\sqrt{s_{\mathrm{NN}}} = 7.7$ and 14.6 GeV. For events with one Ω, at least three $s\bar{s}$ pairs are produced because of SC. The AMPT results are slightly greater than three, and the slight excess indicates that the other strangeness productions do not significantly affect the number of $s\bar{s}$. Compared with the SM version of AMPT, the default version yields a slightly greater number of $s\bar{s}$ pairs and a smaller Ω formation probability. This correlation is presumably due to differences in the formation dynamics and/or the $s\bar{s}$ phase space. AMPT simulations suggest that numerous strange quarks per event are needed to favorably form an Ω^- hyperon during collisions at lower energies.

Table 3 lists the AMPT calculations for ΔN_K and $\Delta N_{\bar{B}}$ as defined in Eq. (1). Compared with the expectations listed in Table 1, which correspond to the two Ω production scenarios, these numbers indicate that Ω production is likely to receive contributions from both scenarios. The SM version seems to favor the dominance of general associate production, with ΔN_K values close to three and to the lower $\Delta N_{\bar{B}}$ values. This may be explained by the fact that in the SM version, for the Ω^- that do not originate from pair production, the production depends on the s-quark threshold. In addition, in the coalescence version, production does not increase, causing an enhancement in the general associate production scenario.

Strangeness and baryon numbers can be represented by various particle types in the final states of nuclear collision. For example, $\bar{s}$ quarks may exist in K^+ and K^0. The actual distributions of strangeness and baryon numbers in final-state particles may be sensitive to nuclear dynamics and may also depend on the beam energy. Figures 3 and 4 show the AMPT results of the differences in strange hadron yields between Ω^- and non-Ω^- events of Au+Au collisions at 7.7 and 14.6 GeV, respectively. At 7.7 and 14.6 GeV, the correlations between Ω^- and kaons are stronger in the SM version. By contrast, those between Ω^- and anti-hyperons are stronger in the default version. For Ω^- events, the number of kaons is much greater than the number of anti-hyperons, suggesting that the correlations between Ω^- and kaons are much stronger than those between Ω^- and anti-hyperons. According to Table 1, these numbers seem to support the idea that general associate production contributes more significantly to Ω yields in both versions.

3.2 Correlations between $\Omega^{\pm}$ and strange hadrons

We first show the correlations between Ω and strange hadrons as a function of the reduced momentum k^* in the pair rest frame using event mixing normalization. Figure 5 presents the correlation functions for the (a) Ω^--K^+, (b) Ω^--$\bar{\Lambda}$, and (c) Ω^--$\bar{\Xi}^+$ pairs for 0–5% centrality Au + Au collisions at 7.7 GeV. The normalization between the

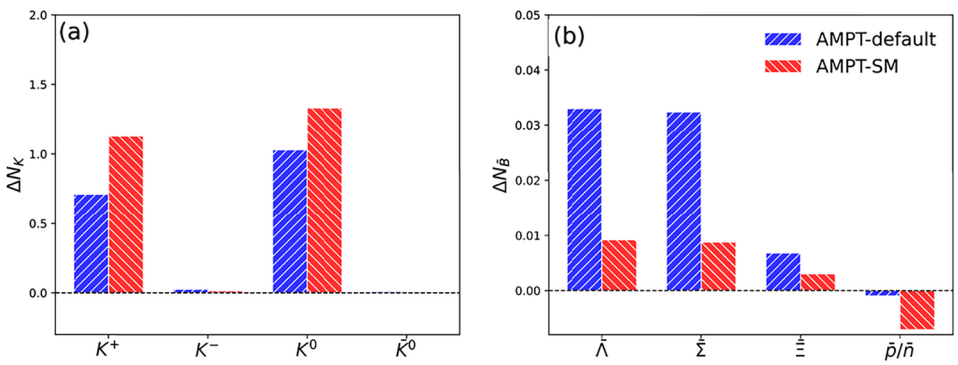

Fig. 3 (Color online) AMPT calculations of the difference in strange hadron yields between Ω^- and non-Ω^- events of Au+Au collisions at 7.7 GeV

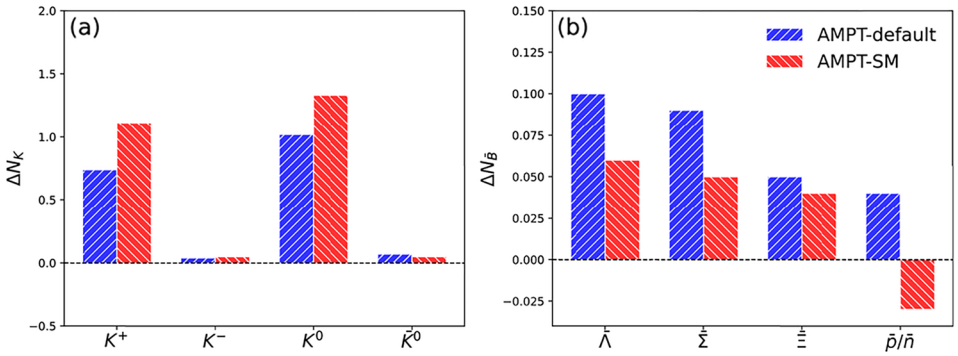

Fig. 4 (Color online) AMPT calculations of the difference in strange hadron yields between Ω^- and non-Ω^- events of Au+Au collisions at 14.6 GeV

Table 1 ΔN_K and $\Delta N_{\bar{B}}$ in the two scenarios for the production of an Ω^-

	ΔN_K	$\Delta N_{\bar{B}}$
General associate production (SC+BNT)	3	0
General pair production (SC)	1, 2, 3	1

Table 2 Differences in the numbers of $s\bar{s}$ pairs in the 0-5% centrality between events with one Ω^- and those without any Ω^- or $\bar{\Omega}^+$

	7.7 GeV	14.6 GeV
AMPT SM	3.22	3.07
AMPT default	3.25	3.16

Table 3 Average numbers of ΔN_K and $\Delta N_{\bar{B}}$ in the 0-5% centrality as defined in Eq. (1)

	7.7 GeV		14.6 GeV	
	ΔN_K	$\Delta N_{\bar{B}}$	ΔN_K	$\Delta N_{\bar{B}}$
AMPT SM	2.46	0.017	2.44	0.119
AMPT default	1.74	0.078	1.76	0.28

same- and mixed-event distributions is determined by the k^* region of 0.6–1.5 GeV/c. A distinct correlation exists between Ω^- and K^+, indicating that SC plays a major role in the Ω^- and K^+ yields with a typical correlation length on the order of less than k^* of 0.5 GeV/c. Ω^- may also be correlated with the anti-hyperons of $\bar{\Lambda}$ and $\bar{\Xi}^+$. However, the current simulated results do not have sufficient statistics to be definitive.

Figure 6 shows (a) Ω^--K^+, (b) Ω^--$\bar{\Lambda}$, and (c) Ω^--$\bar{\Xi}^+$ correlations for the 0–5% centrality Au + Au collisions at 14.6 GeV. The Ω^--K^+ correlation at 14.6 GeV seems to be less prominent than that at 7.7 GeV. This can be explained by our normalization scheme, in which the normalization factor is the number of uncorrelated Ω^--K^+ pairs. More kaons are produced at higher energies, resulting in more uncorrelated kaons pairing with Ω at 14.6 GeV, diluting the correlation between the Ω^--K^+ due to the combinatorial background.

Table 1 shows that the correlation between Ω and anti-hyperons may also be susceptible to the Ω-pair production scenario. The middle and right panels in Figs. 5 and 6 show the Ω^--$\bar{\Lambda}^0$ and Ω^--$\bar{\Xi}^+$ correlation functions, respectively, which were obtained using the event mixing technique at 7.7 and 14.6 GeV, respectively. At both energies, the Ω^--$\bar{\Lambda}^0$ results lack sufficient statistics for a definitive conclusion, whereas some level of Ω^--$\bar{\Xi}^+$

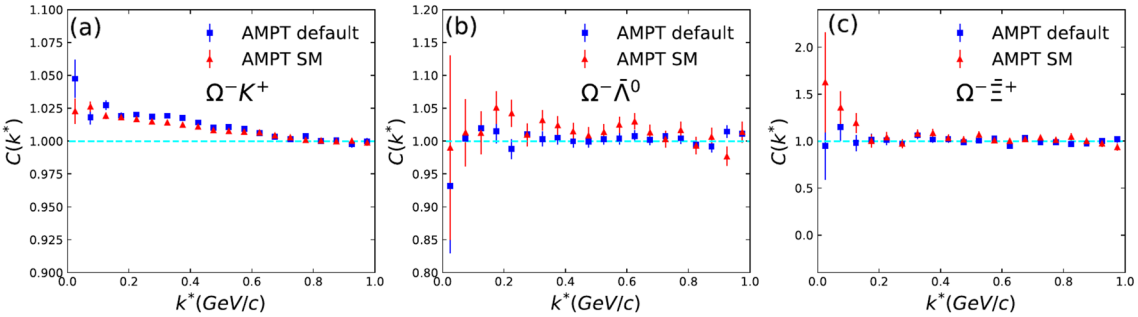

Fig. 5 Correlation functions between Ω^- and strange hadrons using the event mixing normalization in the 0–5% centrality range of Au + Au collisions at 7.7 GeV ($|\eta| < 1$)

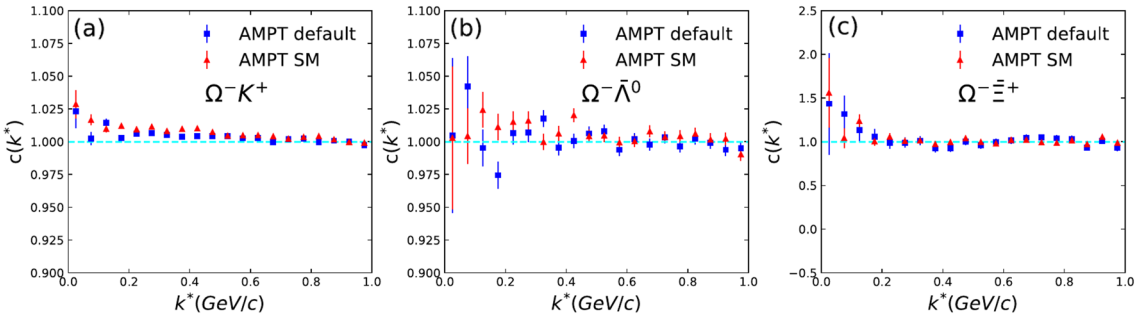

Fig. 6 Correlation functions between Ω^- and strange hadrons using the event mixing normalization in the 0–5% centrality range of Au + Au collisions at 14.6 GeV ($|\eta| < 1$)

correlation may exist. However, no significant difference appears between Ω^--$\bar{\Xi}^+$ and $\bar{\Omega}^+$-Ξ^-, which is similar to the Ω-K results.

For both beam energies, no significant difference exists in the observed correlations between the two AMPT hadronization schemes. It appears that the correlations using the event mixing technique are sensitive only to the kinematic region where SC produces $s\bar{s}$ pairs. However, the magnitude differences, as listed in Table 3, are not quantitatively reflected in the measured correlations due to the normalization scheme. We explore the CBS correlations within the same event framework and background subtraction scheme.

Our goal is to use the $\bar{\Omega}^+$-K^- correlation (general pair production only) as a reference for comparison with the Ω^--K^+ correlation. For each CBS correlation, we again select events with one Ω^- or $\bar{\Omega}^+$ from 0–5% of the most central collisions. As described in Eq. (3), the combinatorial background of the Ω^--K^+ correlation is modeled by the $\bar{\Omega}^+$-K^+ correlation based on events with one $\bar{\Omega}^+$. $\bar{\Omega}^+$ and K^+ both contain $\bar{s}$ quarks, and the narrow centrality bin makes the $\bar{\Omega}^+$-K^+ correlation a good candidate for the combinatorial background in the Ω^--K^+ correlation. Similarly, we can also use the difference between $\bar{\Omega}^+$-K^- and Ω^--K^- to calculate the $\bar{\Omega}^+$-K^- correlation, which represents contributions from only the SC. In summary, Ω^--K^+ includes both BNT and SC dynamics, whereas $\bar{\Omega}^+$-K^- includes only the SC. Therefore, any difference between Ω^--K^+ and $\bar{\Omega}^+$-K^- correlations will be sensitive to the net BNT dynamics, which are absent in general pair production.

Figure 7 shows the CBS correlations for (left) Ω^--K^+ and (right) $\bar{\Omega}^+$-K^- at 7.7 and 14.6 GeV, respectively. The correlations are shown as functions of k^*, rapidity difference (Δy), and transverse momentum difference (Δp_{T}) in the three rows, respectively. At 7.7 GeV, the two AMPT versions exhibit clear differences. Compared with the SM version, the default version shows a stronger $\bar{\Omega}^+$-K^- correlation, presumably indicating a stronger and more localized SC. For the Ω^--K^+ correlation, which is sensitive to both the SC and BNT dynamics while the total magnitudes (integral) are similar between the two AMPT versions, the correlation shapes differ as a function of both k^* and Δp_{T}. In the SM version, the coalescence formation mechanism and BNT dynamics seem to yield a narrower correlation function between Ω^- and K^+.

At 14.6 GeV (Fig. 7), the difference between the two hadronization schemes is relatively small. The shape difference in the correlation as a function of k^* and Δp_T is much less prominent than at 7.7 GeV. The CBS correlations at 7.7 and 14.6 GeV suggest that the event-level Ω^--K^+ correlation is stronger than that of the $\bar{\Omega}^+$-K^-. In general pair production, Ω^- does not carry a net baryon number transported from the colliding nuclei. Because $\bar{\Omega}^+$ is produced only by pair production, whereas Ω^- can be produced in both scenarios, the stronger Ω^--K^+ correlation indicates significant contributions of general associate production to Ω^- production at both beam energies. Particularly at 7.7 GeV, general associate production seems to contribute more to Ω^- production in the SM version, as the difference in correlation amplitudes between Ω^--K^+ and $\bar{\Omega}^+$-K^- becomes noticeably larger.

Figure 8 shows the CBS correlations between Ω and $\bar{\Lambda}$ and their anti-particle pairs as a function of three kinematic variables in 0–5% of the most central Au + Au collisions at 7.7 and 14.6 GeV, respectively. In addition to strangeness and baryon number conservation that govern the correlations between Ω^- and $\bar{\Lambda}$, the $\bar{\Omega}^+$-Λ correlations are also sensitive to BNT dynamics. At 7.7 GeV, the default version of AMPT displays stronger correlations than the SM version.

For both AMPT versions, the Ω^--$\bar{\Lambda}$ correlations are much weaker than those of $\bar{\Omega}^+$-Λ, which is consistent with the fact that $\bar{\Omega}^+$ is produced only through general pair production. The default version also indicates a greater discrepancy between $\bar{\Omega}^+$-Λ and Ω^--$\bar{\Lambda}$, which suggests a more significant contribution from general pair production, complementary to the difference between the Ω^--K^+ and $\bar{\Omega}^+$-K^- results. At 14.6 GeV, the $\bar{\Omega}^+$-Λ correlations (right column in Fig. 9) are also higher than those of Ω^--$\bar{\Lambda}$ (left column in Fig. 9) by approximately one order of magnitude. However, no significant difference appears between the two AMPT versions at this energy level.

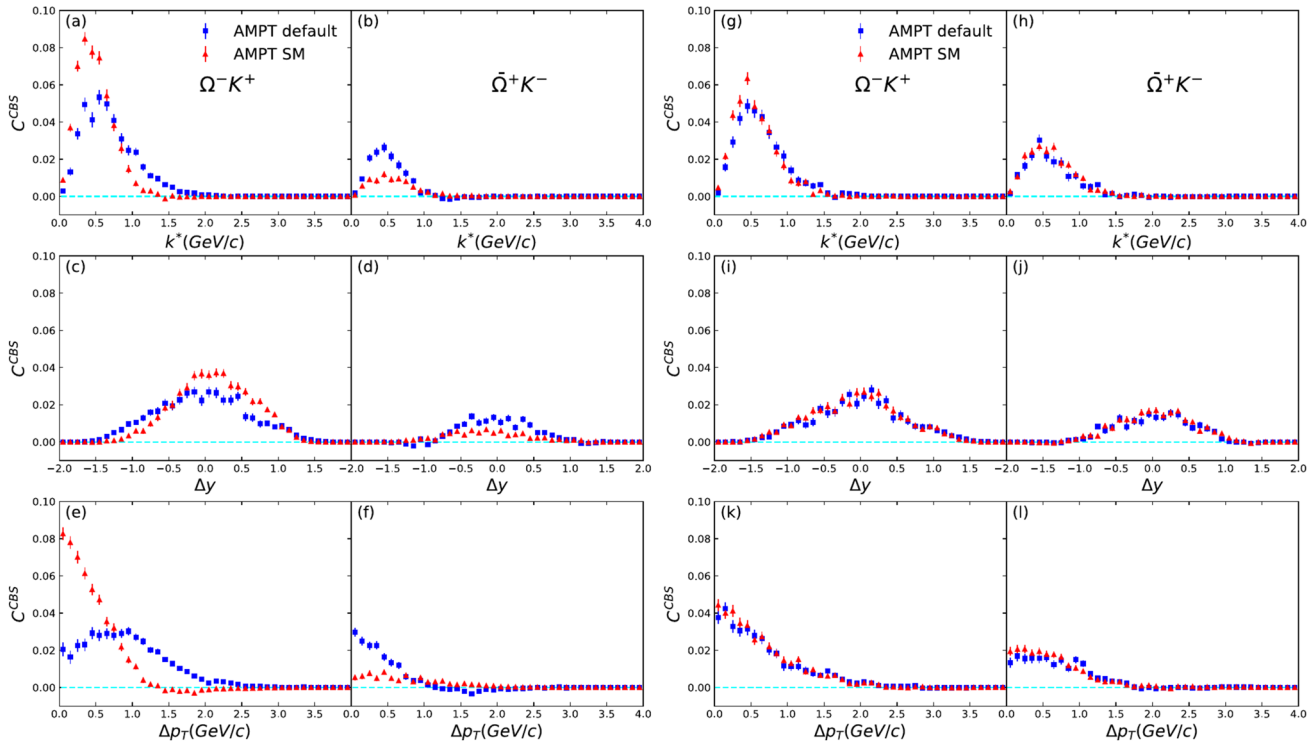

Fig. 7 CBS correlations between $\Omega^-\left(\bar{\Omega}^+\right)$ and kaons in 0–5% of the most central Au + Au collisions at 7.7 and 14.6 GeV ($|\eta| < 1$). The left and right columns show the results of $C^{\mathrm{CBS}}_{\Omega^-K^+}$ and $C^{\mathrm{CBS}}_{\bar{\Omega}^+K^-}$ at 7.7 and 14.6 GeV, respectively

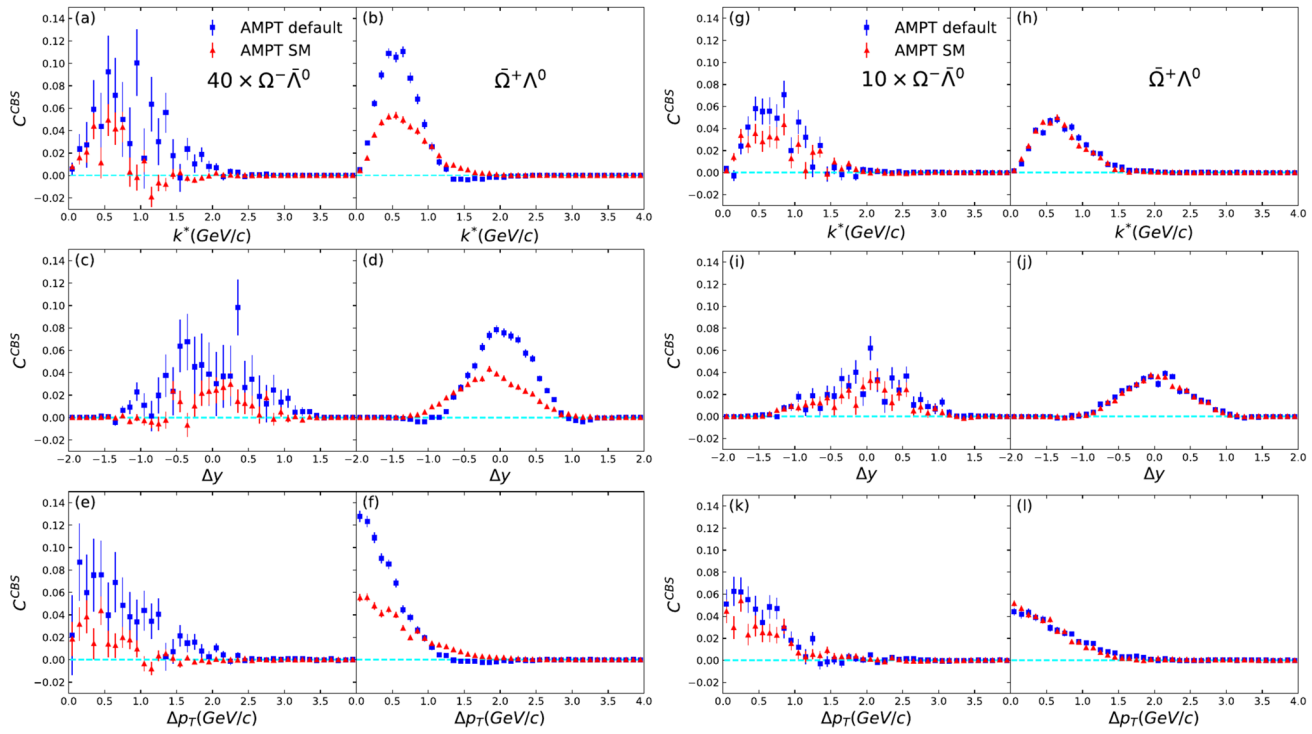

Fig. 8 CBS correlations between $\Omega^-\left(\bar{\Omega}^+\right)$ and $\bar{\Lambda}(\Lambda)$ in 0–5% of the most central Au + Au collisions at 7.7 and 14.6 GeV ($|\eta| < 1$). The left columns show the results of $40 \times C^{\mathrm{CBS}}_{\Omega^-\bar{\Lambda}}$ and $C^{\mathrm{CBS}}_{\bar{\Omega}^+\Lambda}$ at 7.7 GeV. The right shows the results of $10 \times C^{\mathrm{CBS}}_{\Omega^-\bar{\Lambda}}$ and $C^{\mathrm{CBS}}_{\bar{\Omega}^+\Lambda}$ at 14.6 GeV

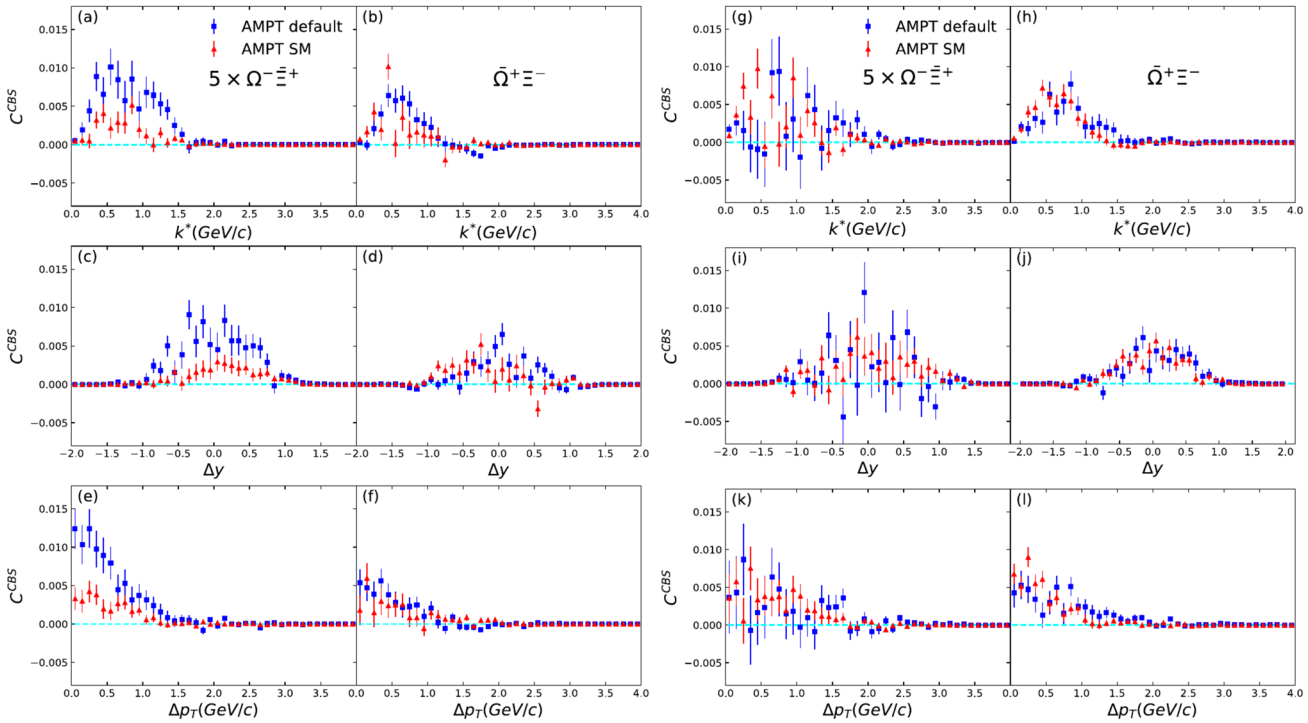

Fig. 9 CBS correlations between $\Omega^{-}\left(\bar{\Omega}^{+}\right)$ and $\bar{\Xi}^{+}(\Xi^{-})$ in 0–5% of the most central Au + Au collisions at 7.7 and 14.6 GeV ($|\eta| < 1$). The left and right columns show the results of $5 \times C^{\mathrm{CBS}}_{\Omega^{-}\bar{\Xi}^{+}}$ and $C^{\mathrm{CBS}}_{\bar{\Omega}^{+}\Xi^{-}}$ and of those at 14.6 GeV, respectively

Figure 9 shows the CBS correlations between Ω and $\bar{\Xi}$ as functions of the three kinematic variables in 0–5% of the most central Au + Au collisions at 7.7 and 14.6 GeV, respectively. At both beam energies, the stronger $\bar{\Omega}^{+}$-Ξ^{-} correlations relative to Ω^{-}-$\bar{\Xi}^{+}$ are consistent with the fact that general pair production provides a larger contribution to the $\bar{\Omega}^{+}$ production than to that of Ω^{-}. At 7.7 GeV, the difference in the Ω^{-}-$\bar{\Xi}^{+}$ correlations between the two AMPT versions suggests that the default version generates a larger contribution from general pair production to Ω^{-} production. At 14.6 GeV, the $\bar{\Omega}^{+}$-Ξ^{-} correlations are still stronger than those of Ω^{-}-$\bar{\Xi}^{+}$, but no significant difference appears between the two versions.

4 Summary

The Ω production in nuclear collisions at the RHIC BES involves the dynamics of baryon number transport, SC, and baryon number conservation. To investigate these effects, we used the AMPT model with both the default and string-melting versions to simulate central Au+Au collisions at 7.7 and 14.6 GeV and showed that Ω^{-}-K^{+} and Ω^{-}-anti-hyperon correlations are sensitive to the dynamics. In particular, we considered two generic Ω production scenarios: one with three $\bar{s}$ quarks in kaons (general associate production) and Ω carrying a net baryon number, and the other with baryon pair production of Ω and anti-baryon with $\bar{s}$ quarks in anti-hyperon and kaons (general pair production). Both scenarios were shown to be constrained by strangeness and baryon number conservation, where only the former is sensitive to net baryon number transport. The AMPT simulations showed that in Au+Au collisions, both scenarios contribute to Ω production, and general associate production becomes more important from 14.6 to 7.7 GeV. The shapes of the correlations can also be sensitive to the hadronization schemes in the default and string-melting versions of the AMPT model. Experimental measurements of these correlations and comparisons with our AMPT simulation results could greatly advance our understanding of baryon transport dynamics and the effects of strangeness and baryon number conservation on Ω production and possibly enable future experimental studies on exotic baryon transport mechanisms such as gluon junction interactions.

Author Contributions All authors contributed to the study conception and design. Material preparation, data collection and analysis were performed by Weijie Dong, Xiaozhou Yu and Xiatong Wu. The first draft of the manuscript was written by Weijie Dong and all authors commented on previous versions of the manuscript. All authors read and approved the final manuscript.

Data Availability The data that support the findings of this study are openly available in Science Data Bank at https://cstr.cn/31253.11.sciencedb.18474 and https://doi.org/10.57760/sciencedb.18474.

Declarations

Conflict of interest Huan-Zhong Huang is an editorial board member for Nuclear Science and Techniques and was not involved in the editorial review, or the decision to publish this article. All authors declare that there are no Conflict of interest.

References

1. P. Koch, B. Müller, J. Rafelski, Strangeness in relativistic heavy ion collisions. Phys. Rep. **142**, 167 (1986). https://doi.org/10.1016/0370-1573(86)90096-7
2. J. Adams et al., (STAR), Experimental and theoretical challenges in the search for the quark-gluon plasma: The star collaboration's critical assessment of the evidence from RHIC collisions. Nucl. Phys. A **757**, 102 (2005). https://doi.org/10.1016/j.nuclphysa.2005.03.085
3. S.V. Afanasiev et al., (NA49), Energy dependence of pion and kaon production in central Pb+ Pb collisions. Phys. Rev. C. **66**, 054902 (2002). https://doi.org/10.1103/PhysRevC.66.054902
4. C. Alt et al., (NA49), Pion and kaon production in central Pb+ Pb collisions at 20 A and 30 A GeV: Evidence for the onset of deconfinement. Phys. Rev. C. **77**, 024903 (2008). https://doi.org/10.1103/PhysRevC.77.024903
5. J. Adams et al., (STAR), Scaling properties of hyperon production in Au+ Au collisions at $\sqrt{s_{\rm NN}}$ = 200 GeV. Phys. Rev. Lett. **98**, 062301 (2007). https://doi.org/10.1103/PhysRevLett.98.062301
6. B.I. Abelev et al., (STAR), Energy and system size dependence of ϕ meson production in Cu+ Cu and Au+ Au collisions. Phys. Lett. B. **673**, 183–191 (2009). https://doi.org/10.1016/j.physletb.2009.02.037
7. J. Rafelski, B. Müller, Strangeness production in the quark-gluon plasma. Phys. Rev. Lett. **48**, 1066 (1982). https://doi.org/10.1103/PhysRevLett.48.1066
8. F. Antinori et al., (WA97), Production of strange and multistrange hadrons in nucleus nucleus collisions at the SPS. Nucl. Phys. A **661**, 130 (1999). https://doi.org/10.1016/S0375-9474(99)85015-5
9. B.I. Abelev et al. (STAR), Enhanced strange baryon production in Au + Au collisions compared to p + p at $\sqrt{s_{NN}}$ = 200 GeV. Phys. Rev. C **77**, 044908 (2008). https://doi.org/10.1103/PhysRevC.77.044908
10. B.B. Abelev et al. (ALICE), Multi-strange baryon production at mid-rapidity in Pb-Pb collisions at $\sqrt{s_{NN}}$ = 2.76 TeV. Phys. Lett. B **728**, 216 (2014), [Erratum: Phys. Lett. B 734, 409–410 (2014)]. https://doi.org/10.1016/j.physletb.2014.05.052
11. J. Adam et al. (ALICE), Enhanced production of multi-strange hadrons in high-multiplicity proton-proton collisions. Nature Phys. **13**, 535 (2017). https://doi.org/10.1038/nphys4111
12. H. Hecke, H. Sorge, N. Xu, Evidence of early multi-strange hadron freeze-out in high energy nuclear collisions. Nucl. Phys. A. **661**, 493–496 (1999). https://doi.org/10.1103/PhysRevLett.81.5764
13. A. Shor, ϕ-meson production as a probe of the Quark-Gluon Plasma. Phys. Rev. Lett. **54**, 1122 (1985). https://doi.org/10.1103/PhysRevLett.54.1122
14. S. Takeuchi, K. Murase, T. Hirano et al., Effects of hadronic rescattering on multistrange hadrons in high-energy nuclear collisions. Phys. Rev. C **92**, 044907 (2015). https://doi.org/10.1103/PhysRevC.92.044907
15. B. Mohanty, N. Xu, Probe of the QCD phase diagram with ϕ -mesons in high-energy nuclear collisions. J. Phys. G Nucl. Part. Phys. **36**, 064022 (2009). https://doi.org/10.1088/0954-3899/36/6/064022
16. S.W. Lan, S.S. Shi, Anisotropic flow in high baryon density region. Nucl. Sci. Tech. **33**, 21 (2022). https://doi.org/10.1007/s41365-022-01006-0
17. Z. Zhu, Y. Q. Zhao, and D. Hou, QCD phase structure from holographic models. Nucl. Tech. (in Chinese) **46**, 040007 (2023). https://doi.org/10.11889/j.0253-3219.2023.hjs.46.040007
18. Y. Yin, The best framework for exploring the QCD phase diagram: progress summary. Nucl. Tech. (in Chinese) **46**, 040010 (2023). https://doi.org/10.11889/j.0253-3219.2023.hjs.46.040010
19. Y. Du, C. M. Li, C. Shi, et al. Review of QCD phase diagram analysis using effective field theories. Nucl. Tech. (in Chinese) **46**, 040009 (2023). https://doi.org/10.11889/j.0253-3219.2023.hjs.46.040009
20. Y.J. Ye, J.H. Chen, Y.G. Ma et al., Ω and ϕ in Au+ Au collisions at $\sqrt{s_{NN}}$ 200 and 1.15 GeV from a multiphase transport model. Chin. Phys. C **41**, 084101 (2017). https://doi.org/10.1088/1674-1137/41/8/084101
21. X.H. Jin, J.H. Chen, Y.G. Ma et al., Ω and ϕ production in Au+ Au collisions at $\sqrt{s_{NN}}$ = 1.15 and 7.7 GeV in a dynamical quark coalescence model. Nucl. Sci. Tech. **29**, 54 (2018). https://doi.org/10.1007/s41365-018-0393-1
22. J.H. Chen, J. Fu, H.Z. Huang, Y.G. Ma, Parton distributions at hadronization from bulk dense matter produced in Au+ Au collisions at $\sqrt{s_{NN}}$ = 200 GeV. Phys. Rev. C. **78**, 034907 (2008). https://doi.org/10.1088/0954-3899/36/6/064016
23. X. Luo, N. Xu, Search for the QCD critical point with fluctuations of conserved quantities in relativistic heavy-ion collisions at RHIC: an overview. Nucl. Sci. Tech. **28**, 112 (2017). https://doi.org/10.1007/s41365-017-0257-0
24. J. Adam et al. (STAR), Strange hadron production in Au+Au collisions at $\sqrt{s_{\rm NN}}$ = 7.7, 11.5, 19.6, 27, and 39 GeV. Phys. Rev. C **102**, 034909 (2020). https://doi.org/10.1103/PhysRevC.102.034909
25. W. Busza, A.S. Goldhaber, Nuclear stopping power. Phys. Lett. B **139**, 235 (1984). https://doi.org/10.1016/0370-2693(84)91070-0
26. W. Busza, R. Ledoux, Energy deposition in high-energy proton-nucleus collisions. Ann. Rev. Nucl. Part. Sci. **38**, 119 (1988). https://doi.org/10.1146/annurev.ns.38.120188.001003
27. H. Z. Huang, in Aps Centennial Meeting '99: Selected topics on baryon transport in nuclear collisions, in Heavy Ion Physics From Bevalac To RHIC-Proceedings Of The Relativistic Heavy Ion Symposium (World Scientific, 1999) p. 3
28. J. Brandenburg, N. Lewis, P. Tribedy *et al.*, Search for baryon junctions in photonuclear processes and isobar collisions at RHIC. (2022). arXiv:2205.05685

29. W. Lv, Y. Li, X. Li, *et al.* Correlations of Baryon and Charge Stopping in Heavy Ion Collisions (2024). arXiv:2309.06445
30. D. Kharzeev, Can gluons trace baryon number? Phys. Lett. B **378**, 238 (1996). https://doi.org/10.1016/0370-2693(96)00435-2
31. Z.W. Lin, L. Zheng, Further developments of a multi-phase transport model for relativistic nuclear collisions. Nucl. Sci. Tech. **32**, 113 (2021). https://doi.org/10.1007/s41365-021-00944-5
32. Z.W. Lin, C.M. Ko, B.A. Li, B. Zhang, S. Pal, Multiphase transport model for relativistic heavy ion collisions. Phys. Rev. C **72**, 064901 (2005). https://doi.org/10.1103/PhysRevC.72.064901
33. X.N. Wang, Role of multiple minijets in high-energy hadronic reactions. Phys. Rev. D **43**, 104 (1991). https://doi.org/10.1103/PhysRevD.43.104
34. X.N. Wang, M. Gyulassy, HIJING: a monte carlo model for multiple jet production in pp, pA, and AA collisions. Phys. Rev. D **44**, 3501 (1991). https://doi.org/10.1103/PhysRevD.44.3501
35. X.N. Wang, M. Gyulassy, Systematic study of particle production in p+p collisions via the HIJING model. Phys. Rev. D **45**, 844 (1992). https://doi.org/10.1103/PhysRevD.45.844
36. X.N. Wang, M. Gyulassy, Gluon shadowing and jet quenching in A+A collisions at $\sqrt{s}$= 200A GeV. Phys. Rev. Lett. **68**, 1480 (1992). https://doi.org/10.1103/PhysRevLett.68.1480
37. B. Andersson, G. Gustafson, G. Ingelman, T. Sjöstrand, Parton fragmentation and string dynamics. Phys. Rep. **97**, 31 (1983). https://doi.org/10.1016/0370-1573(83)90080-7
38. B.A. Li, C.M. Ko, Formation of superdense hadronic matter in high energy heavy-ion collisions. Phys. Rev. C **52**, 2037 (1995). https://doi.org/10.1103/PhysRevC.52.2037
39. J. Adam et al., (STAR), Phi meson production in Au + Au and p+p collisions at $\sqrt{s_{NN}}$ = 200 GeV. Phys. Lett. B **612**, 181–189 (2005). https://doi.org/10.1016/j.physletb.2004.12.082